

# Topography of the Potential Energy Hypersurface and Criteria for Fast-Ion Conduction in Perovskite-Related $A_2B_2O_5$ Oxides

Svein Stølen,<sup>\*,†</sup> Chris E. Mohn,<sup>†</sup> P. Ravindran,<sup>‡</sup> and Neil L. Allan<sup>‡</sup>

Department of Chemistry and Centre for Nanotechnology and Materials Science, University of Oslo, Postbox 1033 Blindern, N0315 Oslo, Norway, and School of Chemistry, University of Bristol, Cantock's Close, Bristol BS8 1TS, U.K.

Received: February 8, 2005; In Final Form: April 20, 2005

We discuss the importance of the topography of the potential energy hypersurface for the ionic conductivity of perovskite-related  $A_2B_2O_5$  oxides. A correlation between the energetic preference of the cations for different coordination geometries and the ionic conductivity is proposed based on a first principles periodic density functional theory study of selected possible structures for  $Ba_2In_2O_5$ ,  $Sr_2Fe_2O_5$ ,  $Sr_2Mn_2O_5$ , and  $La_2Ni_2O_5$ . There are a large number of low-energy local minima on the potential energy hypersurfaces of the two first compounds due to an energetic preference for  $BO_4$  tetrahedra. Tetrahedral environments are energetically unfavorable for Mn(III) in  $Sr_2Mn_2O_5$  and for Ni(II) in  $La_2Ni_2O_5$ , and the number of low-energy configurations is relatively low in these two cases. Consistent with our findings, in contrast to  $Sr_2Fe_2O_5$  and  $Ba_2In_2O_5$ ,  $Sr_2Mn_2O_5$  and  $La_2Ni_2O_5$  do not exhibit transitions to disordered phases on heating, and there appear to be no reports of enhanced ionic conductivity for these compounds. Thus we suggest that the possibility of many different oxygen orderings associated with a variety of low-energy connectivity schemes within tetrahedral layers such as in the brownmillerite-based structures of  $Sr_2Fe_2O_5$  and  $Ba_2In_2O_5$  is a prerequisite for high ionic conductivity in perovskite-related  $A_2B_2O_5$  oxides.

## Introduction

The complexity of grossly disordered structures hinders fundamental understanding of the functional properties of many classes of advanced materials. Links between the dynamic structure, thermodynamic behavior, and ionic and electronic conductivity are central themes in contemporary solid-state science, and disordered materials remain a challenge to both experiment and theory. Present models most often describe the structures and thermodynamics of disordered nonstoichiometric oxides in terms of random distributions of oxygen atoms and oxygen vacancies on the available oxygen sites and their dynamic behavior in terms of single or correlated ion-jump mechanisms.<sup>1,2</sup>

Recently we proposed an alternative interpretation focusing on the local structure present in the disordered state.<sup>3</sup> Configurations that were energetically accessible at a given temperature were thought of as representing snapshots of small regions of the disordered material, and the average structure observed experimentally (at high temperature) was interpreted as a time and spatial average of the different local environments. This local structure interpretation has implications also for our understanding of the ionic conduction. Transition paths connecting thermally accessible low-energy crystallographically nonequivalent configurations (CNCs) using the climbing-image nudge-elastic-band method<sup>4</sup> suggest a collective mechanism for ion transport in the fast-ion conductor  $Ba_2In_2O_5$  in which different energetically accessible local structural environments play important roles.<sup>3,5</sup>

The present contribution highlights the importance of the topography of the potential energy hypersurface of the solid

and suggests structural criteria, in turn related to the electronic structure, for fast ionic conduction through a study of selected configurations for  $Sr_2Mn_2O_5$ ,  $Sr_2Fe_2O_5$ , and  $La_2Ni_2O_5$ . Each of these compounds adopts a different perovskite-related structure. While the structure of  $Sr_2Mn_2O_5$  is based on corner-sharing square pyramids (Figure 1a),<sup>6–8</sup>  $Sr_2Fe_2O_5$  adopts a brownmillerite-type structure in which alternate layers contain corner-sharing  $FeO_6$  octahedra and  $FeO_4$  tetrahedra (Figure 1b).<sup>9</sup> The structure of  $La_2Ni_2O_5$  is built from alternate layers of corner-sharing  $NiO_6$  octahedra and square planar entities (Figure 1c).<sup>10,11</sup> Structural order–disorder transitions to cubic perovskites with significant ionic conductivity are observed in  $Sr_2Fe_2O_5$  at 1120 K,<sup>12</sup> in isostructural  $Ca_2Fe_2O_5$  at 973 K, and in  $Ba_2In_2O_5$  at 1140–1230 K.<sup>14,15</sup> In contrast,  $Sr_2Mn_2O_5$ , isostructural  $Ca_2Mn_2O_5$ , and  $La_2Ni_2O_5$  do not undergo transitions to disordered phases at these temperatures, and there appear to be no reports of enhanced ionic conductivity for these compounds. Our purpose in this paper is to examine the reasons for this different behavior, and we present a correlation linking structure to ion conduction. In our previous work on  $Ba_2In_2O_5$ , we calculated the energies of all possible oxygen orderings in a  $2 \times 2 \times 2$  supercell (36 atoms)<sup>3</sup> and determined energy barriers to oxygen transport.<sup>5</sup> Our purpose in this paper is to establish a structure–activity relationship between ionic conductivity and structure by considering a selection of the oxygen orderings obtained for  $Ba_2In_2O_5$ ,<sup>3,5</sup> avoiding explicit (spin-polarized) calculations of the energy barriers to migration that are exceedingly expensive.

## Computational Details

We have carried out structural optimizations (with respect to *all* unit cell dimensions and basis atom coordinates) of  $Sr_2Mn_2O_5$ ,  $Sr_2Fe_2O_5$ , and  $La_2Ni_2O_5$  in the three different structural

\* Corresponding author. E-mail: svein.stolen@kjemi.uio.no.

<sup>†</sup> University of Oslo.

<sup>‡</sup> University of Bristol.

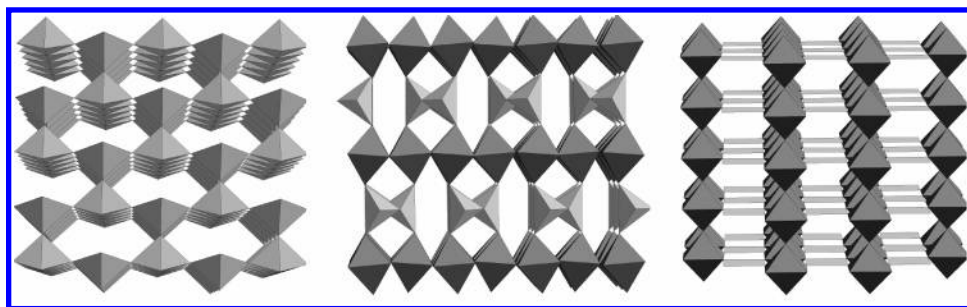


**Figure 1.** Polyhedral representation of low-temperature crystal structures of (a)  $\text{Sr}_2\text{Mn}_2\text{O}_5$ ,<sup>6–8</sup> (b)  $\text{Sr}_2\text{Fe}_2\text{O}_5$ ,<sup>9</sup> and (c)  $\text{La}_2\text{Ni}_2\text{O}_5$ .<sup>10–11</sup>

arrangements given in Figure 1 using periodic density functional theory (DFT) within the generalized gradient approximation (GGA), with a sufficiently large basis of projected augmented plane waves (a constant energy cutoff of 700 eV), as implemented in the Vienna ab initio simulation program (VASP).<sup>16,17</sup> In addition, in the case of  $\text{Sr}_2\text{Fe}_2\text{O}_5$  where tetrahedral coordination is favorable, test calculations have been carried out for selected low-energy configurations structurally related to the brownmillerite-type structure but with different oxygen ordering in the tetrahedral layers. Spin-polarized calculations were carried out to check that the correct ground state properties were obtained for the experimentally observed structures for each compound. In addition, the magnetically ordered structures represent the paramagnetic high-temperature state better than non-spin-polarized calculations. Ferromagnetic and selected antiferromagnetic orderings were considered. The  $k$ -space integration was increased until a satisfactory convergence of energy was reached.

## Results and Discussion

Previously for  $\text{Ba}_2\text{In}_2\text{O}_5$  we optimized all distributions of oxygen vacancies over the possible oxygen sites in a  $2 \times 2 \times 2$  supercell and also calculated energy barriers between selected configurations. We obtained a total of 21 500 relaxed local energy minima on the potential energy hypersurface.<sup>3,5</sup> Many of these were high in energy, and only a fraction of the local structural entities were shown to contribute significantly to the disordered state at other than very high temperatures. Thus, here, for  $\text{Sr}_2\text{Mn}_2\text{O}_5$ ,  $\text{Sr}_2\text{Fe}_2\text{O}_5$ , and  $\text{La}_2\text{Ni}_2\text{O}_5$ , only a selection of structures are considered. The energies of the three different structures in Figure 1 (those adopted by  $\text{Sr}_2\text{Mn}_2\text{O}_5$ ,  $\text{Sr}_2\text{Fe}_2\text{O}_5$ , and  $\text{La}_2\text{Ni}_2\text{O}_5$ , respectively) for each of the three compounds are shown in Figure 2b, where they are also compared with the low-energy portion of the energy vs degeneracy plot for  $\text{Ba}_2\text{In}_2\text{O}_5$  (Figure 2a).<sup>3,5</sup>

All energies plotted are those of the lowest energy states obtained in spin-polarized calculations. Details of the calculated crystal and magnetic structures and the magnetic moments of the lowest energy structures of  $\text{Sr}_2\text{Mn}_2\text{O}_5$ ,  $\text{Sr}_2\text{Fe}_2\text{O}_5$ , and  $\text{La}_2\text{Ni}_2\text{O}_5$  are given in Tables 1 and 2 together with selected experimental data. The observed structures and magnetic orderings are lowest in energy, and the unit cell dimensions are in good agreement with experiment. The atomic coordinates also agree well with observation, and the calculated structures thus represent the interatomic distances well. All three ground state configurations are predicted to be insulators in agreement with experiment. Note that the calculated electronic structure of  $\text{La}_2\text{Ni}_2\text{O}_5$  is very sensitive to the starting point of the structural optimization. If we take the monoclinic crystal structure<sup>11</sup> as a starting point, the correct insulating behavior is obtained. If we instead use the previously reported and closely related orthorhombic structure<sup>18</sup> as a starting point, we get a metallic state

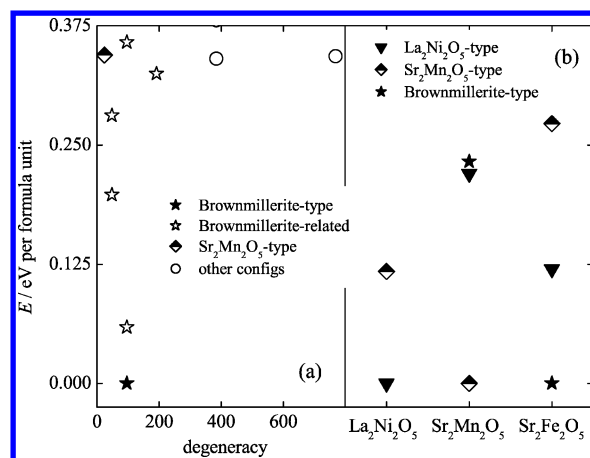


**Figure 2.** (a) Low-energy portion of energy–degeneracy plot for  $2 \times 2 \times 2$  cell of  $\text{Ba}_2\text{In}_2\text{O}_5$ .<sup>3,5</sup> (b) Energies of selected CNCs for  $\text{La}_2\text{Ni}_2\text{O}_5$ ,  $\text{Sr}_2\text{Mn}_2\text{O}_5$ , and  $\text{Sr}_2\text{Fe}_2\text{O}_5$ . All energies are relative to those of the lowest energy structure for each system, assigned a value of zero. Note that the brownmillerite-type structure for  $\text{La}_2\text{Ni}_2\text{O}_5$  is 0.72 eV above the ground state and thus beyond the scale used on the vertical axis in (b).

with slightly higher energy. The magnetic order and spin state of the B-site cation for the higher energy structures are given in Table 3. For our present purposes, these magnetically ordered structures and their corresponding energies represent the paramagnetic high-temperature state sufficiently well since the energy differences between the magnetically ordered structures and the paramagnetic states are small compared to the energy scale in Figure 2.

Large differences in the relative stability of the various structure types are evident. While structures containing  $\text{BO}_4$  tetrahedra are energetically favorable for  $\text{Sr}_2\text{Fe}_2\text{O}_5$  and  $\text{Ba}_2\text{In}_2\text{O}_5$ , this is not so for  $\text{Sr}_2\text{Mn}_2\text{O}_5$  and  $\text{La}_2\text{Ni}_2\text{O}_5$ . Consistent with the molecular structural chemistry of Mn(III) and Ni(II), the energetic preference in these compounds is for square pyramidal and square planar coordination, respectively. For  $\text{Sr}_2\text{Mn}_2\text{O}_5$ , the  $\text{La}_2\text{Ni}_2\text{O}_5$ -type and  $\text{Sr}_2\text{Fe}_2\text{O}_5$ -type structures, both of which contain 50% 4-coordinate Mn, lie close in energy to each other, 0.22 and 0.23 eV per formula unit above the ground state. For  $\text{La}_2\text{Ni}_2\text{O}_5$ , the  $\text{Sr}_2\text{Mn}_2\text{O}_5$ -type structure is 0.12 eV per formula unit above the ground state; the  $\text{Sr}_2\text{Fe}_2\text{O}_5$ -type structure is still higher in energy by an additional 0.60 eV per formula unit above the  $\text{Sr}_2\text{Mn}_2\text{O}_5$ -type structure, and is therefore beyond the scale of the vertical axis in Figure 2b. For  $\text{Sr}_2\text{Fe}_2\text{O}_5$ , in contrast, the two other structural types are closer in energy, lying 0.12 eV ( $\text{La}_2\text{Ni}_2\text{O}_5$ -type) and 0.27 eV per formula unit ( $\text{Sr}_2\text{Mn}_2\text{O}_5$ -type) above the ground state.

We have shown earlier that the square planar geometry is very unfavorable for In and that the  $\text{La}_2\text{Ni}_2\text{O}_5$ -type structure is very high in energy for  $\text{Ba}_2\text{In}_2\text{O}_5$ .<sup>3</sup> Nevertheless, a number of other CNCs have rather low energies; see Figure 2a. These are all close relatives of the lowest energy brownmillerite-type

**TABLE 1: Calculated and Experimental Values for the Unit Cell Dimensions of the Lowest Energy Structures of  $\text{Sr}_2\text{Mn}_2\text{O}_5$ ,  $\text{Sr}_2\text{Fe}_2\text{O}_5$ , and  $\text{La}_2\text{Ni}_2\text{O}_5$** 

	ref
$\text{Sr}_2\text{Mn}_2\text{O}_5$	
$a = 5.526 \text{ \AA}, b = 10.882 \text{ \AA}, c = 3.834 \text{ \AA}$	this work
$a = 5.5060(2) \text{ \AA}, b = 10.7458(4) \text{ \AA}, c = 3.8057(1) \text{ \AA}$	7
$a = 5.5307(4) \text{ \AA}, b = 10.7829(8) \text{ \AA}, c = 3.8145(3) \text{ \AA}$	8
$\text{Sr}_2\text{Fe}_2\text{O}_5$	
$a = 5.635 \text{ \AA}, b = 16.154 \text{ \AA}, c = 5.530 \text{ \AA}$	this work
$a = 5.672(1) \text{ \AA}, b = 15.59(2) \text{ \AA}, c = 5.527(1) \text{ \AA}$	9
$\text{La}_2\text{Ni}_2\text{O}_5$	
$a = 5.5499 \text{ \AA}, b = 7.5455 \text{ \AA}, c = 11.1162 \text{ \AA}, \alpha = 86.23^\circ, \beta = 89.86^\circ, \gamma = 86.26^\circ$	this work
$a = 5.5308 \text{ \AA}, b = 7.4703 \text{ \AA}, c = 11.0616 \text{ \AA}, \alpha = 87.25^\circ, \beta = 89.65^\circ, \gamma = 87.25^\circ$	11 <sup>a</sup>

<sup>a</sup> The reported setting is transformed to a triclinic cell in order to describe the proper magnetic structure.

**TABLE 2: Calculated and Experimental Magnetic Properties of the Lowest Energy structures of  $\text{Sr}_2\text{Mn}_2\text{O}_5$ ,  $\text{Sr}_2\text{Fe}_2\text{O}_5$ , and  $\text{La}_2\text{Ni}_2\text{O}_5$** 

	magnetic order	magnetic structure	magnetic moment	ref
$\text{Sr}_2\text{Mn}_2\text{O}_5$	AF	(0, 0, 1/2)	$\mu = 3.25 \mu_B$	this work
	AF	(0, 0, 1/2)	$\mu_x = 0.5(2) \mu_B$	7
			$\mu_y = 3.20(6) \mu_B$	7
	AF	(0, 0, 1/2)	$\mu_y = 3.44 \mu_B$	7
$\text{Sr}_2\text{Fe}_2\text{O}_5$				
sublattice 1	AF	G-type	$\mu(\text{Fe}_{\text{oct}}) = 3.50 \mu_B$	this work
sublattice 2	AF		$\mu(\text{Fe}_{\text{tet}}) = -3.44 \mu_B$	this work
sublattice 1	AF		$\mu_z(\text{Fe}_{\text{oct}}) = 3.85(7) \mu_B$	9
sublattice 2	AF		$\mu_z(\text{Fe}_{\text{tet}}) = -3.67(8) \mu_B$	9
$\text{La}_2\text{Ni}_2\text{O}_5$				
sublattice 1	AF	(1/2, 1/2, 0)	$\mu(\text{Ni}_{\text{oct}}) = 1.248 \mu_B$	this work
sublattice 2	nonmagnetic		$\mu(\text{Ni}_{\text{sq,plan}}) = 0 \mu_B$	this work
sublattice 1	AF	(1/2, 1/2, 0)	$\mu_x(\text{Ni}_{\text{oct}}) = 0.5(2) \mu_B$	11
			$\mu_z(\text{Ni}_{\text{oct}}) = 1.9(3) \mu_B$	11
sublattice 2	nonmagnetic		$\mu(\text{Ni}_{\text{sq,plan}}) = 0 \mu_B$	11

**TABLE 3: Calculated Magnetic Properties for Higher Energy Structure Types for  $\text{Sr}_2\text{Mn}_2\text{O}_5$ ,  $\text{Sr}_2\text{Fe}_2\text{O}_5$ , and  $\text{La}_2\text{Ni}_2\text{O}_5$** 

compound	structure type	magnetic order	spin state of B-site cation
$\text{Sr}_2\text{Mn}_2\text{O}_5$	$\text{Sr}_2\text{Fe}_2\text{O}_5$	antiferromagnetic	high-spin Mn(III)
	$\text{La}_2\text{Ni}_2\text{O}_5$	antiferromagnetic	high-spin Mn(III)
$\text{Sr}_2\text{Fe}_2\text{O}_5$	$\text{Sr}_2\text{Mn}_2\text{O}_5$	antiferromagnetic	high-spin Fe(III)
	$\text{La}_2\text{Ni}_2\text{O}_5$	ferromagnetic	high-spin Fe(III)
$\text{La}_2\text{Ni}_2\text{O}_5$	$\text{Sr}_2\text{Fe}_2\text{O}_5$	nonmagnetic	
	$\text{Sr}_2\text{Fe}_2\text{O}_5$	nonmagnetic	

structure, differing in that they contain other types of oxygen orderings or connectivity patterns within the tetrahedral layers, as discussed in detail in ref 3. Test calculations show that such brownmillerite-related CNCs are relatively low in energy also for  $\text{Sr}_2\text{Fe}_2\text{O}_5$ , in agreement with earlier force-field calculations,<sup>19</sup> and thus a number of different low-energy CNCs exist also for this compound. The brownmillerite-related CNCs are not considered for  $\text{La}_2\text{Ni}_2\text{O}_5$  and  $\text{Sr}_2\text{Mn}_2\text{O}_5$  because they will be even higher in energy than the brownmillerite-type itself.

The stability of the different local structural entities has important implications for possible mechanisms of ion transport in these materials. Ionic movement is necessarily highly restricted by the local symmetry and the energy changes involved in its alteration. For  $\text{Ba}_2\text{In}_2\text{O}_5$ , as shown in Figure 2a, and also  $\text{Sr}_2\text{Fe}_2\text{O}_5$  there are energetically accessible excited states, which involve different connectivity patterns within the tetrahedral layers. In previous work we have shown that there are collective, low-energy pathways between these different arrangements, consistent with enhanced ionic conductivity at higher temperatures.<sup>3</sup>

The present calculations together with the absence of order–disorder transitions in  $\text{Sr}_2\text{Mn}_2\text{O}_5$  and  $\text{La}_2\text{Ni}_2\text{O}_5$  and of any

reports of enhanced ionic conductivity for these compounds suggest there are no energetically accessible excited configurations for these compounds due to the relative stabilization of the ground state structure. The stabilization of the ground state ensures that the activation energy for any single-jump oxygen diffusion mechanism must be high in these compounds due to the accompanying change in Mn or Ni coordination.

On the basis of our calculations, we propose a simple structure–activity relationship connecting local structure and disorder, and hence ion conduction. The existence of low-lying excited configurations involving tetrahedrally coordinated atoms appears to be crucial. These give a large number of possible oxygen positions that are important for collective mechanisms involving strongly correlated motions of sets of tetrahedra. In this context it is worth noting that in the  $2 \times 2 \times 2$  cell for  $\text{Ba}_2\text{In}_2\text{O}_5$  there are around 650 configurations with 50% tetrahedrally and 50% octahedrally coordinated In atoms, around 300 configurations based solely on 5-fold coordination, and only around 100 configurations containing 50% square planar entities and 50% octahedral entities. Thus, the number of configurations involving different sorts of connectivity patterns within the tetrahedral layers of brownmillerite-related structures is considerably larger than the number of configurations solely based on square pyramids or on square planar and octahedral entities. This is due to a large number of possible sites within the O(3) plane when distributing tetrahedra in the brownmillerite-type structure. The result is a large number of structurally related connectivity patterns and many low-energy transition pathways for oxygen ion transport.

A characteristic of compounds containing tetrahedra is their rather large molar volume compared to compounds with the same stoichiometry that contain square planar or square



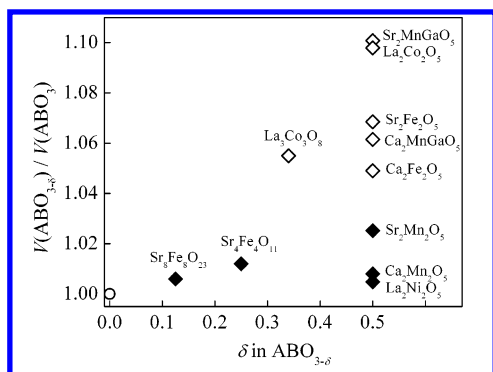


**Figure 3.** Ratio of volumes of reduced compounds  $ABO_{3-\delta}$  to those of corresponding non-oxygen-deficient perovskites  $ABO_3$  ( $V(ABO_{3-\delta})/V(ABO_3)$ ) for a number of systems. The open diamonds denote compounds in which tetrahedral coordination is energetically favorable; the filled diamonds are compounds where square planar or square pyramidal structural entities are favored.

pyramidal structural entities. Figure 3 shows the ratio of the volumes of a range of reduced compounds  $ABO_{3-\delta}$  to those of the corresponding non-oxygen-deficient perovskites  $ABO_3$  ( $V(ABO_{3-\delta})/V(ABO_3)$ ). The open diamonds denote compounds in which tetrahedral coordination is energetically favorable; the filled diamonds are compounds where square planar or square pyramidal structural entities are favored. While  $SrFeO_{3-\delta}$  compounds with  $\delta = 0.125$  ( $Sr_8Fe_8O_{23}$ ) and  $0.25$  ( $Sr_4Fe_4O_{11}$ ), both of which contain square pyramidal entities, have rather small volumes relative to that of  $SrFeO_3$ ,  $SrFeO_{2.50}$ , which adopts the brownmillerite-type structure with layers of tetrahedra, has a high relative volume. Furthermore, while  $Ca_2Mn_2O_5$  and  $Sr_2Mn_2O_5$  both have structures built exclusively from corner-sharing square pyramids and thus have low relative volumes, partial substitution of Mn by Ga or Al leads to brownmillerite-type structures with high relative volumes.<sup>20,21</sup> Ga and Al both have strong site preferences for tetrahedral coordination, and in  $Ca_2MnGaO_5$ ,  $Sr_2MnGaO_5$ , and also  $Ca_2MnAlO_5$  and  $Sr_2MnAlO_5$  Mn occupies the octahedral site and Ga or Al the tetrahedral site. Thus structures in which tetrahedra are energetically preferred are relatively open; compare our simple structure–activity relationship connecting local structure and ion conduction in which the existence of low-lying excited configurations involving tetrahedrally coordinated atoms appears to be crucial. The openness of the structure is affected not only by the coordination preference of the B cation but also by the A cations, and Sammells and co-workers<sup>22</sup> have used the concept of lattice free volume (the unit cell volume minus the total volume of the constituent ions) to rationalize the ionic conductivity of perovskite-type oxides. Larger free volumes for a given substitution degree are often associated with higher ionic conductivities. This argument has recently been used to rationalize the increase in ionic conductivity<sup>23</sup> of  $Ba_2In_2O_5$  when there is partial substitution of Ba with Sr or La. In contrast, the presence of an additional cation which either generates a local structural environment other than tetrahedral in the tetrahedral layer, or which creates disorder within the ordered tetrahedra due to size mismatch between different types of B atoms, may lead to a decrease in the conductivity. It has, for example, been shown that partial substitution of In by Ga in  $Ba_2In_2O_5$  decreases the ionic conductivity of the cubic high-temperature phase.<sup>24</sup>

Further work is in progress to address the effects of substitution on the A and B sites.

## Conclusion

We have proposed a structure–activity relationship that connects local structure, disorder, and ion conduction. This emphasizes the importance of the topography of the potential energy hypersurface for understanding fast-ion conduction. A high density of low-lying excited configurations is a prerequisite for high ionic conductivity, and perovskite-related  $A_2B_2O_5$  oxides containing B atoms that have energetic preference for tetrahedral coordination geometry are especially interesting. We suggest that the possibility of many different oxygen orderings associated with a variety of low-energy connectivity schemes within tetrahedral layers of such compounds (as in the brownmillerite-based structures of  $Sr_2Fe_2O_5$  and  $Ba_2In_2O_5$ ) results in the requested high density of low-lying excited configurations and thus in many low-energy transition pathways for oxygen ion transport.

**Acknowledgment.** This work was funded by Norsk Forskningsråd (Project No. 142995/432). Computational facilities were made available through grants of computer time for the Program for Supercomputing, Norway.

## References and Notes

- (1) Hull, S. *Rep. Prog. Phys.* **2004**, 67, 1233.
- (2) Keen, D. A. *J. Phys.: Condens. Matter* **2002**, 14, R819.
- (3) Mohn, C. E.; Allan, N. L.; Freeman, C. L.; Ravindran, P.; Stølen, S. *J. Solid State Chem.* **2005**, 178, 346.
- (4) Henkelman, G.; Jonsson, H. *J. Chem. Phys.* **2000**, 113, 9978.
- (5) Mohn, C. E.; Allan, N. L.; Freeman, C. L.; Ravindran, P.; Stølen, S. *Phys. Chem. Chem. Phys.* **2004**, 6, 3052.
- (6) Caignaert, V.; Nguyen, N.; Hervieu, M.; Raveau, B. *Mater. Res. Bull.* **1985**, 20, 479.
- (7) Caignaert, V. *J. Magn. Magn. Mater.* **1997**, 166, 117.
- (8) Mori, T.; Inoue, K.; Kamegashira, N.; Yamaguchi, Y.; Ohoyama, K. *J. Alloys Compd.* **2000**, 296, 92.
- (9) Hodges, J. P.; Short, S.; Jorgensen, J. D.; Xiong, X.; Dabrowski, B.; Mini, S. M.; Kimball, C. W. *J. Solid State Chem.* **2000**, 151, 190.
- (10) Vidyasagar, K.; Reller, A.; Gopalakrishnan, J.; Rao, C. N. R. *Chem. Commun.* **1985**, 7.
- (11) Alonso, J. A.; Martinez-Lope, M. J.; Garcia-Munoz, J. L.; Fernandez-Diaz, M. T. *J. Phys.: Condens. Matter* **1997**, 9, 6417.
- (12) Haavik, C.; Bakken, E.; Norby, T.; Stølen, S.; Atake, T.; Tojo, T. *Dalton Trans.* **2003**, 361.
- (13) Berastegui, P.; Eriksson, S.-G.; Hull, S. *Mater. Res. Bull.* **1999**, 34, 303.
- (14) Adler, S. B.; Reimer, J. A.; Baltisberger, J.; Werner, U. *J. Am. Chem. Soc.* **1994**, 116, 675.
- (15) Berastegui, P.; Hull, S.; Garcia-Garcia, F. J.; Eriksson, S. G. *J. Solid State Chem.* **2002**, 164, 119.
- (16) Kresse, G.; Hafner, J. *Phys. Rev. B* **1993**, 47, 558.
- (17) Kresse, G.; Joubert, J. *Phys. Rev. B* **1999**, 59, 1758.
- (18) Moriga, T.; Usaka, O.; Nakabayashi, I.; Kinouchi, T.; Kikkawa, S.; Kanamaru, F. *Solid State Ionics* **1995**, 79, 252.
- (19) Bakken, E.; Allan, N. L.; Barron, T. H. K.; Mohn, C. E.; Todorov, I. T.; Stølen, S. *Phys. Chem. Chem. Phys.* **2003**, 5, 2237.
- (20) Abakumov, A. M.; Alekseeva, A. M.; Rozova, M. G.; Antipov, E. V.; Lebedev, O. I.; van Tendeloo, G. *J. Solid State Chem.* **2003**, 174, 319.
- (21) Abakumov, A. M.; Rozova, M. G.; Pavlyuk, B. Ph.; Lobanov, M. V.; Antipov, E. V.; Lebedev, O. I.; van Tendeloo, G.; Sheptyakov, B. V.; Balagurov, A. M.; Bouree, F. *J. Solid State Chem.* **2001**, 158, 100.
- (22) Sammells, A. F.; Cook, R. L.; White, J. H.; Osborne, J. J.; MacDuff, R. C. *Solid State Ionics* **1992**, 52, 111.
- (23) Kakinuma, K.; Yamamura, H.; Haneda, H.; Atake, T. *Solid State Ionics* **2002**, 154–155, 571.
- (24) Yao, T.; Uchimoto, Y.; Kinuhata, M.; Inagaki, T.; Yoshida, H. *Solid State Ionics* **2000**, 132, 189.